32nd URSI GASS, Montreal, 19–26 August 2017

A Two-Cylinder Based Polarized MIMO Channel Model

Ruisi He*(1)(2), Gordon L. Stüber(2), Bo Ai(1), and Zhangdui Zhong(1)
(1) State Key Laboratory of Rail Traffic Control and Safety, Beijing Jiaotong University, Beijing, 100044, China
(2) School of Electrical and Computer Engineering, Georgia Institute of Technology, Atlanta, 30332, USA
Email: ruisi.he@bjtu.edu.cn

Abstract

In this paper, a polarized Multiple-Input Multiple-Output (MIMO) channel model is proposed by using a geometrical theory based on the "two-cylinder" reference model. The modeling method reveals MIMO channel depolarization and provides a mechanism for computing cross-polarization discrimination (XPD) analytically. The XPD of single-bounced at the transmitter side mode in the polarized MIMO model is analytically discussed, and numerical simulation is conducted to address the impacts of scatterer distribution on XPD. It is found that the resulting XPD of the polarized MIMO channel depends on the MIMO sub-channel index and array orientation. This should be carefully considered in multi-polarized antenna system design.

1 Introduction

Channel depolarization has attracted considerable attention as it significantly affects multi-polarized antenna system performance. Channel depolarization between a transmitter (TX) and a receiver (RX) is mainly caused by the plane waves that arrive at the RX via scattering objects [1], and channel polarization functions are widely used to represent channel depolarization. The radio channel can be characterized in terms of four orthogonal polarization functions f_{VV}, f_{HV}, f_{VH}, and f_{HH}, where H and V refer to horizontal and vertical polarizations, respectively. The degree of depolarization is often measured in terms of the cross-polarization discrimination (XPD), and a few papers have investigated XPD based on channel measurements [2, 3]. However, the above work cannot provide a close-form mathematical model for the simulations of channel depolarization. In [1], a geometrical theory based reference model for narrow-band channel depolarization is proposed, which can be used for quantitatively computing XPD. However, this work is limited to Single-Input Single-Output (SISO) system and cannot be used in the multi-polarized Multiple-Input Multiple-Output (MIMO) system. To clearly address MIMO channel depolarization, in this paper, channel polarization functions are derived by using a geometrical based two-cylinder 3D MIMO statistical model. The approach in [1] is followed, however, the derivations in this paper are modified and extended to a generic MIMO scenario.

2 Polarized MIMO Channel Model

In this paper, a two-cylinder 3D MIMO mobile-to-mobile channel model is considered, as in [4], with channel depolarization. In the following, the model structure and parameters in Fig. 1 are briefly summarized. Linear arrays with L_t TX and L_r RX omnidirectional antenna elements and used. M and N fixed scatterers lie on the surface of two cylinders with radii of R_t and R_r, respectively. The distance between TX and RX, i.e., $\varepsilon_{O'_T O'_R}$, is D, where ε_{XY} indicates the distance between points X and Y in Fig. 1. The spacing intervals between two antenna elements at TX and RX are denoted by d_T and d_R, respectively. Indices of TX and RX antenna elements are denoted by p and q, respectively. Parameters θ_T and θ_R describe the orientations of the TX and RX, ψ_T and ψ_R describe the elevations of TX and RX, $\alpha_{T,m}$ and $\beta_{T,m}$ are the azimuth angle of departure (AAoD) and elevation angle of departure (EAoD), respectively, of TX element O_T for the waves that impinge on the scatterers $S_{T,m}$. Similarly, $\alpha_{R,n}$ and $\beta_{R,n}$ are the azimuth angle of arrival (AAoA) and elevation angle of arrival (EAoA), respectively, of RX element O_R for the waves that received via the scatterer $S_{R,n}$.

Fig. 1 shows that there are generally four different propagation modes: LOS mode, single-bounced at the TX side (SBT) mode, single-bounced at the RX side (SBR) mode, and double-bounced (DB) mode. Due to space limitations, in this paper, the proposed polarized MIMO channel model is only introduced for SBT mode, and the rest results of other modes and further discussions can be found in [5].

Fig. 2 shows the SBT mode where a vertically polarized plane wave $\overrightarrow{V}$ emitted from TX can lead to a horizontally polarized plane wave received at RX. $\overrightarrow{V'}$ is the corresponding polarization vector of $\overrightarrow{V}$ after reflection from a scatterer $S_{T,m}$, which is not entirely vertically polarized anymore and has a cross-polarization component, as shown in Fig. 2. This phenomenon is channel depolarization and is found to depend on the angles in Fig. 2 and other parameters in Fig. 1. Here we name the plane that is defined by TX, RX, and scatterer as a conservation-of-polarization plane as suggested in [1], and θ_V is the angle between $\overrightarrow{V}$ and the line that includes the projection of $\overrightarrow{V}$ onto the conservation-of-

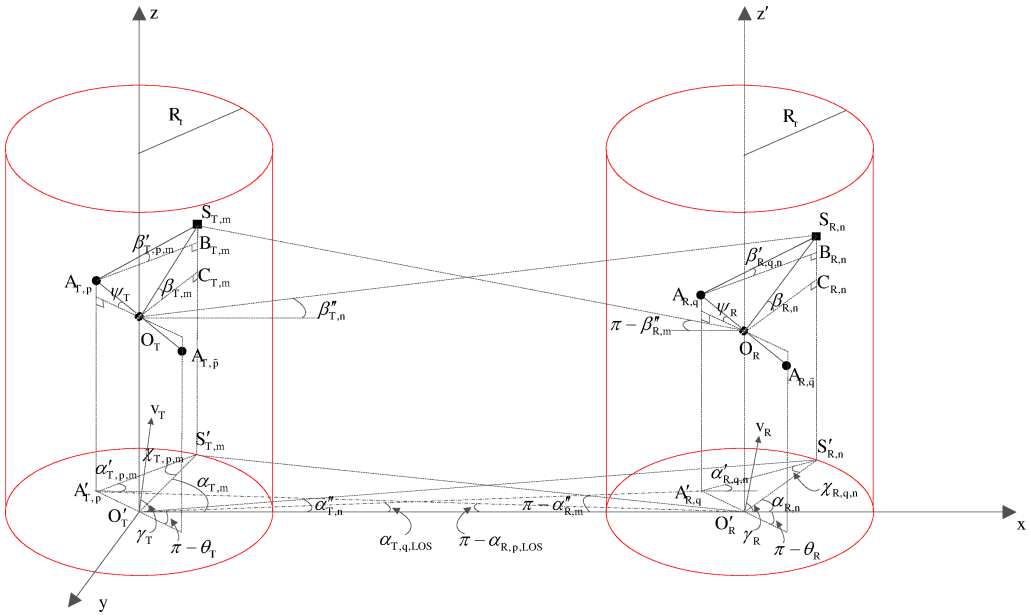

Figure 1. Two-cylinder 3D MIMO channel model with $L_t = L_r = 3$ antenna elements.

polarization plane. Consider a vertically polarized plane wave from TX. By using the geometries of conservation-of-polarization plane in [1], the SBT MIMO channel polarization functions, for the p-q link and the m-th scatterer at TX side can be obtained, as follows

$$f^{\mathrm{SBT}}_{\mathrm{VV},pq,m} = \left|\cos\phi_5\cos\phi_6 - \sqrt{(1-\cos^2\phi_5)(1-\cos^2\phi_6)}\right| \tag{1}$$

$$f^{\mathrm{SBT}}_{\mathrm{HV},pq,m} = \left|\cos\phi_6\sqrt{1-\cos^2\phi_5}+\cos\phi_5\sqrt{1-\cos^2\phi_6}\right| \tag{2}$$

where $|\cdot|$ denotes the absolute value operation. The angles $\cos\phi_5$ and $\cos\phi_6$ can be obtained by using the law of cosines and combining the derivations in [1] with our geometry of 3D MIMO M2M scenario in Figs. 1 and 2, as follows

$$\cos\phi_1 = \frac{\varepsilon^2_{A_{T,p}A_{R,q}} + \varepsilon^2_{B_{T,m}A_{R,q}} - (\varepsilon_{A_{T,p}S_{T,m}}\cos\beta'_{T,p,m})^2}{2\varepsilon_{A_{T,p}A_{R,q}}\varepsilon_{B_{T,m}A_{R,q}}} \tag{3}$$

$$\cos\phi_2 = \frac{\varepsilon^2_{S_{T,m}A_{R,q}} + \varepsilon^2_{B_{T,m}A_{R,q}} - (\varepsilon_{A_{T,p}S_{T,m}}\sin\beta'_{T,p,m})^2}{2\varepsilon_{S_{T,m}A_{R,q}}\varepsilon_{B_{T,m}A_{R,q}}} \tag{4}$$

$$\cos\phi_3 = \frac{\varepsilon^2_{A_{T,p}S_{T,m}} + \varepsilon^2_{A_{T,p}A_{R,q}} - \varepsilon^2_{S_{T,m}A_{R,q}}}{2\varepsilon_{A_{T,p}S_{T,m}}\varepsilon_{A_{T,p}A_{R,q}}} \tag{5}$$

$$\cos\phi_4 = \frac{(\varepsilon_{A_{T,p}S_{T,m}}\cos\beta'_{T,p,m})^2 + \varepsilon^2_{A_{T,p}A_{R,q}} - \varepsilon^2_{B_{T,m}A_{R,q}}}{2\varepsilon_{A_{T,p}S_{T,m}}\varepsilon_{A_{T,p}A_{R,q}}\cos\beta'_{T,p,m}} \tag{6}$$

$$\cos\phi_7 = \frac{\varepsilon^2_{S_{T,m}A_{R,q}} + \varepsilon^2_{A_{T,p}A_{R,q}} - \varepsilon^2_{A_{T,p}S_{T,m}}}{2\varepsilon_{S_{T,m}A_{R,q}}\varepsilon_{A_{T,p}A_{R,q}}} \tag{7}$$

$$\cos\phi_5 = \frac{\cos\phi_1 - \cos\phi_2\cos\phi_7}{\sqrt{(1-\cos^2\phi_2)(1-\cos^2\phi_7)}} \tag{8}$$

$$\cos\phi_6 = \frac{\cos\phi_4 - \cos\beta'_{T,p,m}\cos\phi_3}{\sqrt{(1-\cos^2\beta'_{T,p,m})(1-\cos^2\phi_3)}} \tag{9}$$

For the above equations, distances ε can be calculated by using the law of cosines and the geometries in Figs. 1 and 2. Due to space limitations, in this paper, the calculated equations are not presented, and detailed derivations of the above equations can be found in [5]. With the derived channel polarization functions, the XPD for SBT MIMO scenario can be obtained.

3 XPD

XPD measures depolarization of the propagation environment and is the fundamental parameter for modeling dual-polarized systems. The average XPD for the p-q link is defined as follows

$$\overline{\mathrm{XPD}}_{pq} = \frac{P_{\mathrm{VV},pq}}{P_{\mathrm{HV},pq}} \tag{10}$$

where $P_{\mathrm{VV},pq}$ and $P_{\mathrm{HV},pq}$ are the received powers through the VV and HV channels, respectively. It is noteworthy that as $M,N\to\infty$, discrete departure and arrival angles (in both azimuth and elevation) can be replaced with continuous random variables having a joint probability density function [1]. Therefore, we have

$$P^{\mathrm{SBT}}_{\mathrm{VV/HV},pq} = \frac{A^2_{\mathrm{V},pq}}{2}\eta^{\mathrm{SBT}}\int_{-\pi}^{\pi}\int_{-\beta'_{T,\mathrm{Max}}}^{\beta'_{T,\mathrm{Max}}}(f^{\mathrm{SBT}}_{\mathrm{VV/HV},pq,m})^2 \times p_r(\beta'_T)p_r(\alpha'_T)d\beta'_T d\alpha'_T \tag{11}$$

where $A_{V,pq}$ is the amplitude of the received polarization vector after scattering from a vertically polarized plane wave.

For the azimuth distribution, the von Mises distribution [6] is used, which has been widely employed as it approximates many classical distributions. For the elevation distribution,

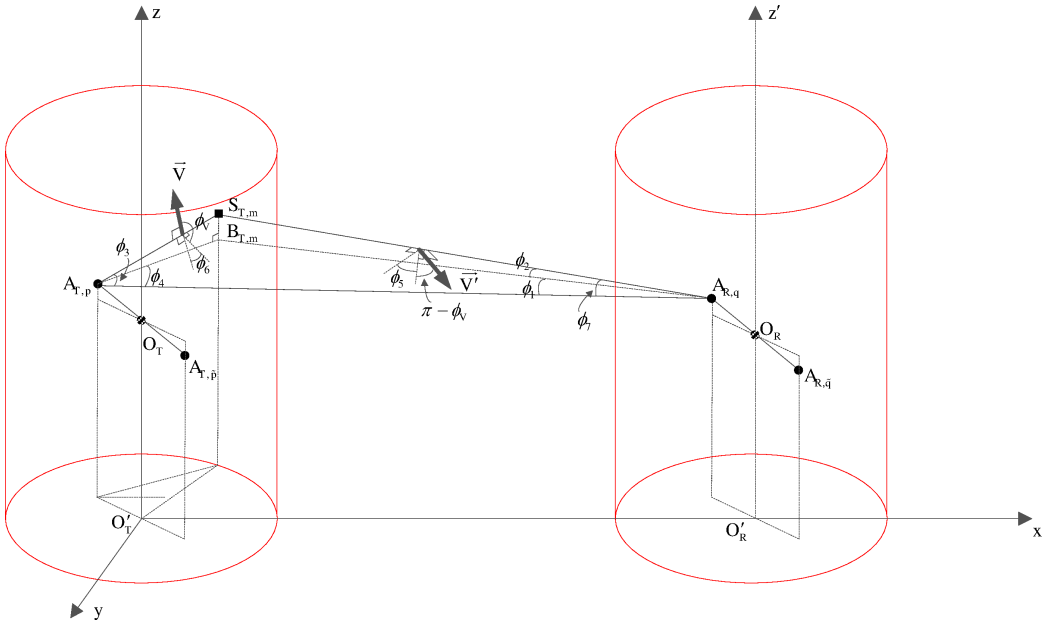

Figure 2. SBT propagation mode for XPD on 3D MIMO channels.

the cosine distribution in [7] is used. The probability density functions of angular distributions are expressed as

$$p_r(\alpha'_T) = \frac{\exp[k_T \cos(\alpha'_T - \mu_T)]}{2\pi I_0(k_T)} \tag{12}$$

$$p_r(\beta'_T) = \frac{\pi}{4\beta'_{T,\mathrm{Max}}} \cos\left(\frac{\pi\beta'_T}{2\beta'_{T,\mathrm{Max}}}\right) \tag{13}$$

where $\alpha'_T \in [-\pi, \pi)$ and $I_0(\cdot)$ is the zero-order modified Bessel function of the first kind, $\mu_T \in [-\pi, \pi)$ is the mean AAoD, k_T indicates the spreads of the scatterers around mean AAoD, and $\beta'_{T,\mathrm{Max}}$ controls the elevation range of scatterers.

4 Numerical Analysis

In this section, based on the above derivations, the impacts of reference model parameters on XPD are numerically analyzed in detail for the SBT mode. This paper only discusses the impact of angular distribution parameters of scatterers on SBT channel depolarization; further investigations of polarized MIMO channels can be found in [5]. The following SBT scenario is considered based on [1, 8]: $f = 2.435$ GHz, $\psi_T = \psi_R = 0°$, $D = 500$ m, $L_t = L_r = 3$, $R_t = R_r = 50$ m, $h_T = h_R = 1.5$ m, $\mu_T = 31.3°$, $\mu_R = 141.7°$, and $d_T = d_R = 60\lambda$. Figs. 3 and 4 show the analytical XPD curves of SBT mode as k_T ranges from 0 to 300, with different $\beta'_{T,\mathrm{Max}}$, p, and q. It is observed that the XPD curve tends to decrease as k_T increases from 0 to 10, and after that the curve increases as k_T increases from 10 to 300, which is similar to the observations in [1]. Furthermore, it is found that a large value of $\beta'_{T,\mathrm{Max}}$ leads to a reduced XPD, which implies that scatterers with large elevation angles lead to strong cross-polarization components. Finally, the results from link $p = q = 1$ are compared with link $p = q = 2$, where a large array spacing of $d_T = d_R = 60\lambda$ is used to clearly show the curve difference. It is found that when $\theta_T = \theta_R = 90°$ in Fig. 3, both links have the same XPD curves, since both links have the same direction (along LOS path); when $\theta_T = 90°$ and $\theta_R = 270°$ in Fig. 4, it is observed that link $p = q = 1$ has a larger XPD compared with link $p = q = 2$. The difference is mainly caused by a different conservation-of-polarization plane and relevant angles. The results in Figs. 3 and 4 show that the polarized MIMO channel is different from SISO channel and should be carefully considered in system design.

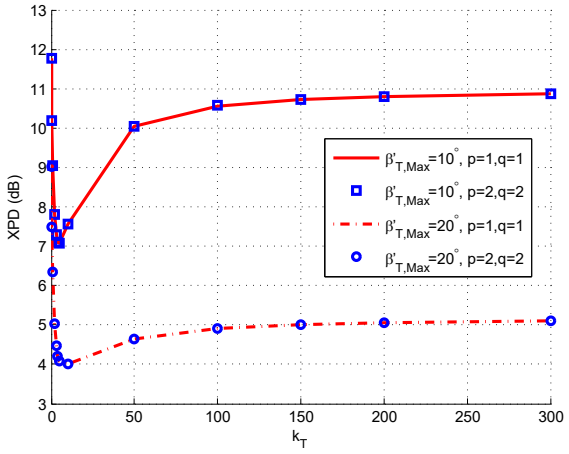

Figure 3. XPD curves of SBT mode for different k_T, where $\theta_T = \theta_R = 90°$.

5 Conclusion

In this paper, a “two-cylinder" based geometrical reference model is proposed for polarized MIMO channels. The

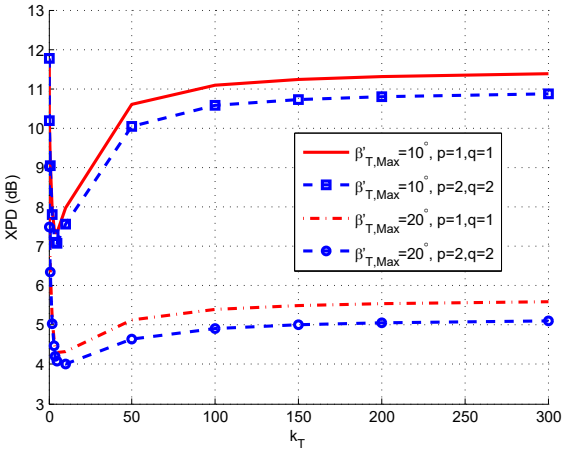

Figure 4. XPD curves of SBT mode for different k_T, where $\theta_T = 90^\circ$ and $\theta_R = 270^\circ$.

mechanisms of channel depolarization are considered in model derivations and analytical methods of calculating XPD for MIMO channel is proposed. The SBT mode of the "two-cylinder" polarized MIMO model is discussed with details and numerical analysis of the impact of angular parameters on XPD is presented. It is found that the polarized MIMO channel is different from polarized SISO channel, and the resulting XPD depends on MIMO sub-channel index and array orientation, which should be carefully considered in system design.

6 Acknowledgements

This work is supported in part by the National Natural Science Foundation of China under Grant 61501020, the State Key Laboratory of Rail Traffic Control and Safety under Grant RCS2016ZJ005, the China Postdoctoral Science Foundation under Grant 2016M591355, the Fundamental Research Funds for the Central Universities (No. 2016JBZ006), the Special Project of Cultivation and Development of Science and Technology Innovation Base in 2015, the National Natural Science Foundation of China under Grant U1334202, the Natural Science Base Research Plan in Shanxi Province of China under Grant 2015JM6320, and the Key Project from Beijing science and Technology Commission under Grant D151100000115004.

References

[1] S.-C. Kwon and G. L. Stüber, "Geometrical theory of channel depolarization," *IEEE Transactions on Vehicular Technology*, **60**, 8, 2011, pp. 3542–3556.

[2] M. Landmann, K. Sivasondhivat, J.-I. Takada, I. Ida, and R. Thoma, "Polarisation behaviour of discrete multipath and diffuse scattering in urban environments at 4.5 GHz," *EURASIP Journal on Wireless Communications and Networking*, **2007**, 1, 2007, pp. 1–16.

[3] V. Erceg, P. Soma, D. Baum, and S. Catreux, "Multiple-input multipleoutput fixed wireless radio channel measurements and modeling using dual-polarized antennas at 2.5 GHz," *IEEE Transactions on Wireless Communications*, **3**, 6, 2004, pp. 2288–2298.

[4] A. G. Zajic and G. L. Stüber, "Three-dimensional modeling, simulation, and capacity analysis of s-paceÍCtime correlated mobile-to-mobile channels," *IEEE Transactions on Vehicular Technology*, **57**, 4, 2008, pp. 2042–2054.

[5] R. He, G. L. Stüber, B. Ai, and Z. Zhong, "Geometrical based statistical modeling for polarized MIMO mobile-to-mobile channels," *to be submitted to IEEE Transactions*, 2017.

[6] A. Abdi, J. A. Barger, and M. Kaveh, "A parametric model for the distribution of the angle of arrival and the associated correlation function and power spectrum at the mobile station," *IEEE Transactions on Vehicular Technology*, **51**, 3, 2002, pp. 425–434.

[7] J. Parsons and A. Turkmani, "Characterisation of mobile radio signals: model description," *IEE Proceedings I-Communications, Speech and Vision*, **138**, 6, 1991, pp. 549–556.

[8] A. G. Zajic and G. L. Stüber, "Wideband MIMO mobile-to-mobile channels: geometry-based statistical modeling with experimental verification," *IEEE Transactions on Vehicular Technology*, **58**, 2, 2009, pp. 517–534.